RSC Advances

PAPER

View Article Online
View Journal | View Issue

Cite this: *RSC Adv.*, 2019, **9**, 31943

Cytotoxic effect, generation of reactive oxygen/nitrogen species and electrochemical properties of Cu(II) complexes in comparison to half-sandwich complexes of Ru(II) with aminochromone derivatives

Paulina Mucha,[a] Pawel Hikisz,[b] Krzysztof Gwoździński,[b] Urszula Krajewska,[c] Andrzej Leniart[d] and Elzbieta Budzisz*[a]

This paper describes the synthesis of new 6-aminoflavone (6AFl (**3**)) and 6-aminochromone (6AC (**4**)) complexes with Cu(II) and Ru(II) ions ($[Cu(6AC)_2Cl_2]$ (**3a**), $[Cu(6AFl)_2Cl_2]$ (**4a**), [Ru(*p*-cymene)(6AC)Cl_2] (**4b**)) and comparison of their properties with the previously described 7-aminoflavone (7AFl (**1**)) and 7-amino-2-methylchromone (7A2MC (**2**)) analogues. The cytotoxic effect of all these complexes against two human leukaemia cell lines (HL-60 and NALM-6), melanoma WM-115 cells and COLO205 cells, is determined. The cytotoxicity of copper(II) complexes, especially $[Cu(6AFl)_2Cl_2]$ (**3a**) was higher than ruthenium(II) complexes with the same ligands. Their cytotoxic potency was also stronger in comparison to the referential agents like cisplatin. The pro-oxidative properties were determined for the most active complexes and their ability to generate ROS (reactive oxygen species)/RNS (reactive nitrogen species) in cancer cells was confirmed. The type of ligand and the chemical structure of the tested complexes had an influence on the level of ROS/RNS generated in cancer cells. The redox properties of the copper complex compounds were evaluated by cyclic voltammetry, and compared with the data for Ru(II) complexes. The reduction and oxidation processes of Ru(III)/Ru(II) and Cu(II)/Cu(I) were described as quasi-reversible.

Received 1st August 2019
Accepted 2nd October 2019

DOI: 10.1039/c9ra05971g

rsc.li/rsc-advances

1. Introduction

Recently, numerous biological studies have examined the properties of natural plant compounds, or phytochemicals. The biological activity of these compounds enables their use as natural healing agents in the treatment of various diseases. *In vitro* and *in vivo* studies have found them to have antioxidant, anti-inflammatory, anticancer and antisclerotic properties among others. The biological activity of flavonoids creates wide possibilities for their use, not only as herbs in traditional medicine, but also as natural medicines in the therapy of various diseases, including cancer. Modern biometalorganic chemistry uses the anticancer properties of flavonoids, mainly aurons and flavones, in combination with metal complexes. An innovative approach to the development of alternative chemotherapeutics contributes to the formation of numerous flavone and chromone derivatives with anticancer effects resulting from the combined properties of the constituent elements: flavonoid/chromone and a metal.[1–4] Recently, compounds containing ruthenium(II)/(III), gold(I)/(III) or copper(II) have been of great interest.[5–8]

The copper ion is an the important species in the body. It is a redox-active transition metal having two main oxidation states, +2 and +1, and coordinates to various heterocyclic ligands such as imidazole nitrogen, amide and amino nitrogen, carboxylate oxygen, cysteine and methionine sulfur donor atoms.[9–14] Although the redoxability of copper is fundamental for the biological activity of a huge number of enzymes, it can become highly dangerous if not accurately regulated. For these reasons, specific proteins are produced to ensure that no copper ions can freely circulate.[15]

Under physiological conditions, ruthenium(II) ions can have three oxidation states: +2, +3 and +4. The energetic barrier of its transition is relatively low so the redox processes can easily occur inside cells. The ruthenium(III) and (IV) ions are more biologically neutral than ruthenium(II) compounds. Hence the Ru(III)/Ru(II) reduction process plays a crucial role in enabling

[a]*Department of Cosmetic Raw Materials Chemistry, Faculty of Pharmacy, Medical University of Lodz, Ul Muszynskiego 1, 90-151 Lodz, Poland. E-mail: elzbieta.budzisz@umed.lodz.pl*

[b]*Department of Molecular Biophysics, Faculty of Biology and Evironmental Protection, University of Lodz, Pomorska 141/143, 90-236, Lodz, Poland*

[c]*Department of Pharmaceutical Biochemistry and Molecular Diagnostics, Faculty of Pharmacy, Medical University of Lodz, Muszynskiego 1, 90-151 Lodz, Poland*

[d]*Department of Electroanalysis and Electrochemistry, Faculty of Chemistry, University of Lodz, Ul Tamka 12, 91-403 Lodz, Poland*

greater anticancer activity. The redox potential of complexes formed with ruthenium ions can be regulated by the choice of ligand.[16–18]

The synthesis and X-ray structures of copper(II) and ruthenium(II) complexes with aminoflavones as ligands and their interesting chemical and biological properties have been described in previous papers.[19,20] However the present paper examines the physicochemical properties of copper(II) and ruthenium(II) complexes with 6-aminoflavone (**3**) and 6-aminochromone (**4**) by the synthesis of new complexes: **3a**, **4a**, **4b**. Due to the potential anticancer activity, low toxicity and high selectivity of all obtained Cu(II) and Ru(II) complexes, their cytotoxicity was compared with that of reference agents like cisplatin, carboplatin, naringenin or quercetin. Our studies also describe the pro-oxidative and electrochemical properties of the most active derivatives by taking measurements of the ROS and RNS generated in human cancer cell lines and by cyclic voltammetry.

2. Results and discussion

2.1. Chemistry

The paper investigates the electrochemical properties, cytotoxic effect and antioxidant activity of copper(II) complexes (series **a**) with 6-/7-aminoflavone/chromone derivatives (Fig. 1) in comparison to their ruthenium analogues (series **b–d**) (Fig. 2).

The new 6-aminoflavone and 6-aminochromone copper(II) (**3a**, **4a**) and ruthenium(II) (**4b**) complexes were synthesized as a reaction between corresponding ligands and copper(II) chloride dihydrate $CuCl_2 \cdot 2H_2O$ (Schemes 1, 2) or [Ru(*p*-cymene)Cl_2]$_2$ (**b**) (Scheme 3) respectively. The ligand : $CuCl_2 \cdot 2H_2O$/[Ru(*p*-cymen)Cl_2]$_2$ molar ratio was 2 : 1 and the reactions were carried in ethyl acetate and chloroform as solvents. All compounds were obtained as coloured solids.

The empirical formulae of the obtained products, which assume 2 : 1 ligand : $CuCl_2$ molar ratio in complexes **3a** and **4a** as well as 1 : 1 ligand : [Ru(*p*-cymen)Cl_2]$_2$ in complex **4b**, were confirmed by elemental analysis. Valuable information about their structure was additionally obtained by IR and ^{1}H, ^{13}C-NMR spectroscopy and mass spectrometry.

2.2. IR analysis

The IR spectroscopy for all examined complexes show significant negative shifts in the area of asymmetric and symmetric *ν*N–H stretching bands displayed from primary amines in the comparison with corresponding free ligands both 6-aminoflavone (**3**) (from 3418 cm^{-1} to 3258 cm^{-1} and from 3343 cm^{-1} to 3123 cm^{-1} in complex **3a**) and 6-aminochromone (**4**) (from 3385 cm^{-1} to 3268 cm^{-1} in complex **4a** and to 3218 cm^{-1} in complex **4b** and from 3234 cm^{-1} to 3139 cm^{-1} in complex **4a** and to 3136 cm^{-1} in complex **4b** respectively). This observation can indicate coordination of the amino groups in all obtained complexes. The absorption bands within 3132–3065 cm^{-1} that are present in all spectra of studied compounds can be the result of the interaction of the 1600 cm^{-1} overtone band and the symmetric *ν*N–H stretching band. The minor shifts of the *ν*C=O band in described complexes suggest that coordination of metal ions by O-atoms is less possible (Table 1).

In comparison, the N-atom coordination in complexes **3a** and **4b** is similar to the analogical Cu(II)-7-aminoflavone (7AFl) complex and the Ru(II)-7-amino-2-methylchromone (7A2MC) complex, respectively, as described previously.[19,20] In the [Cu(7AFl)Cl_2]$_n$ and [Ru(*p*-cymene)(7A2MC)Cl_2] complexes, the *ν*NH bands from stretching asymmetric and symmetric vibrations displayed similar major shifts to the free ligands. The coordination in complex **4a** differs with the correspondent [Cu(7A2MC)$_2$$Cl_2$]$_2$ complex with 7-amino-2-methylchromone as ligand. Additional methyl group in 1-benzopyran-4-one ring and the different position of the amino group caused a very interesting situation where in the same complex one ligand was coordinated by the O-atom and the second was coordinated by an N-atom. In this case, IR data did not provide an unambiguous indication of the type of coordination.[19,20]

2.3. NMR analysis

The ^{1}H-and ^{13}C-NMR spectra of complex **4b** were recorded in DMSO-d_6. The position and intensity of the signals correspond to reagents used in synthesis. In ^{1}H-NMR spectrum signals from six methyl protons of isopropyl group in *p*-cymene were found at 1.19 ppm as doublet and one methanetriyl proton of the same group was observed at 2.84 ppm as a characteristic septet. A singlet observed at 2.09 ppm was assign to three protons of methyl group in *p*-cymene. The resonance of the amino group protons in 6-aminochromone gave a singlet signal at 5.45 ppm. At 5.77 ppm and 5.81 ppm, two doublets from two $H_{2(AA')}$ and two $H_{3(BB')}$ protons respectively in the *p*-cymene ring were also observed. There were also signals ranging from 7.03 ppm to 8.13 ppm as doublets and doublets of doublets, which corresponds to arene protons in chromone arrangement.

In ^{13}C-NMR spectrum signals from carbon atoms of methyl and methanetriyl groups in *p*-cymene were found in a range of

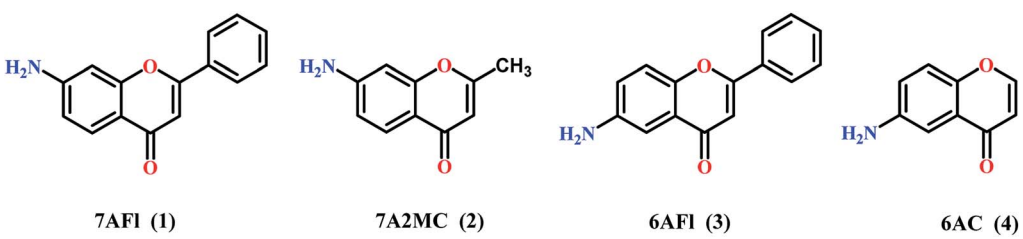

Fig. 1 Structures of the ligands 1–4.

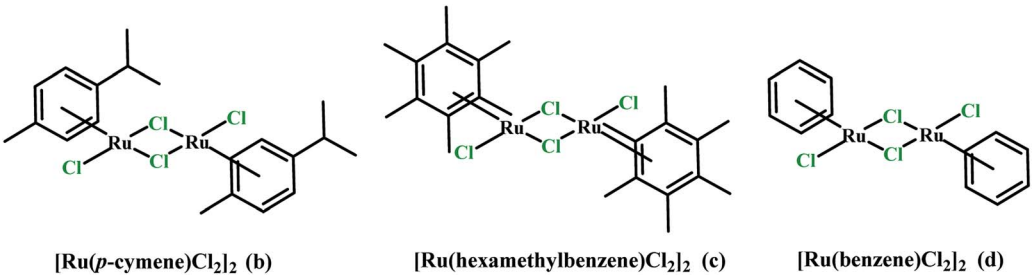

Fig. 2 Structures of the ruthenium(II) dimmers **b–d**.

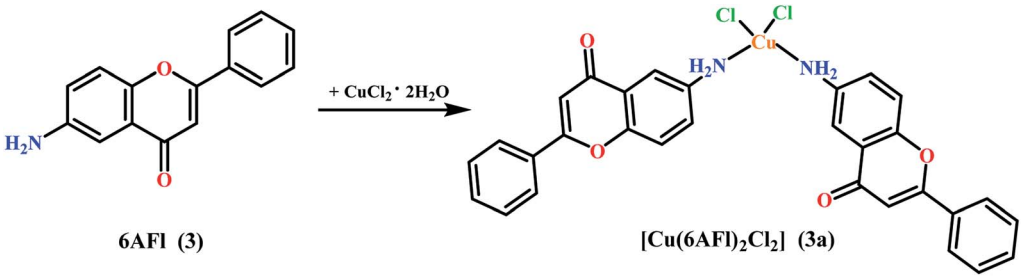

Scheme 1 Synthesis copper(II) complex $[Cu(6AFl)_2Cl_2]$ (**3a**).

18.35 and 30.45 ppm. The area of 85.98–122.11 includes the signals from aromatic carbon atoms from both *p*-cymene and chromone rings. Carbon atoms bonded with heteroatoms in chromone part are shown in the spectrum in a range of 147.03–176.89 ppm.

2.4. ESI-MS

ESI-MS spectrometry was carried out for all new synthesized complexes. The observed parent peak of complex **4b** at m/z = 468.2 was assigned to $[Ru(p\text{-cymene})(6AC)Cl_2]^+$. Structurally informative peaks corresponding to $[2Cu(6AFl)Cl–H]^+$ and $[2Cu(6AC)Cl–H]^+$ were found at m/z = 572.0 for complex **3a** and at m/z = 420.2 for complex **4a** respectively. Presented data confirm the proposed structure and expected 2 : 1 (complexes **3a** and **4a**) and 1 : 1 (complex **4b**) ligand/metal molar ratio.

2.5. Electrochemical properties

Fig. 3 shows a representative CV voltammogram of the copper complex $[Cu(7AFl)Cl_2]$ (**1a**) and ruthenium complex of $[Ru(p\text{-cymene})(6AC)Cl_2]$ (**4b**) registered at a scanning rate of 100 mV s^{-1} in a wide potential range of −2.0 V to +2.0 V. The cyclic voltammograms of other analysed compounds have a very similar shape. The obtained potential–current parameters, including cathodic peak potential (E_{pc}), anodic peak potential (E_{pa}), cathodic peak current (i_{pc}), anodic peak current (i_{pa}), ratio of anodic and cathodic peak currents (i_{pa}/i_{pc}), and the peak-to-peak potentials separation (ΔE_p) are presented in Table 2. For the $[Cu(7AFl)CuCl_2]$ complex (**1a**), the redox system associated with changes in the oxidation state of copper ion, *i.e.* Cu(II)/Cu(I), is visible in the potential range from about −0.10 V to about 0.75 V. It is clearly shown in the CV voltammograms in the range −0.05 V to 0.90 V.

The peaks observed in the anodic region above 0.8 V are mainly related to the oxidation of the ligand fragments. The cyclic voltammogram of the ruthenium complex compound $[Ru(p\text{-cymene})(6AC)Cl_2]$ (**4b**) contain the small anodic peak (i_{pa}) and the cathodic peak (i_{pc}) observed at a potentials −0.10 V and −0.18 V, respectively. These peaks correspond to the oxidation

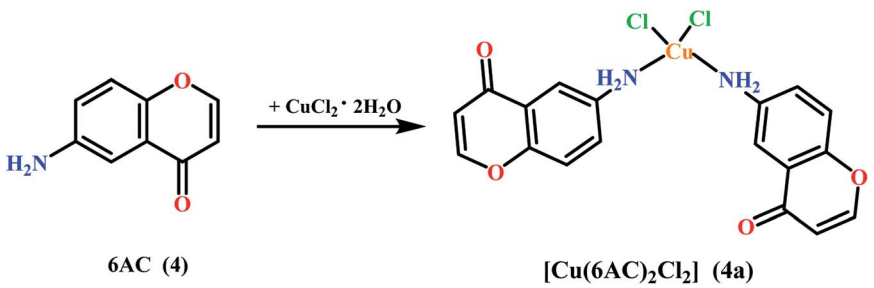

Scheme 2 Synthesis of copper(II) complex $[Cu(6AC)_2Cl_2]$ (**4a**).

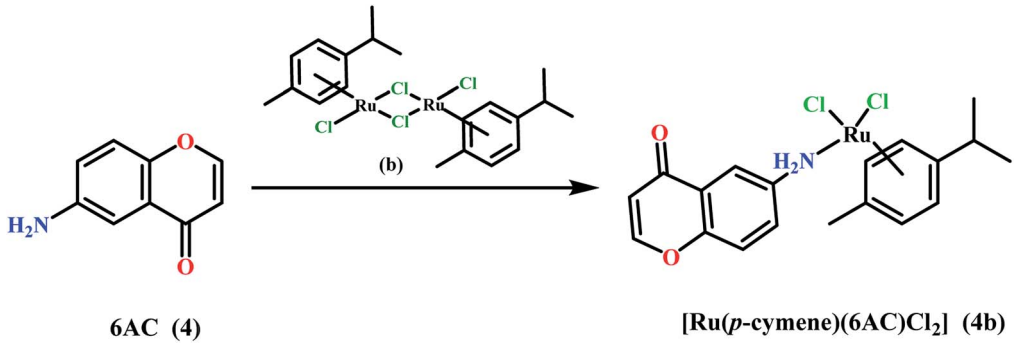

Scheme 3 Synthesis of ruthenium(II) complex [Ru(*p*-cymene)(6AC)Cl_2] (**4b**).

Table 1 IR data for ligands **3** and **4** and complexes **3a**, **4a** and **4b**

Compound	NH_2 (ν cm^{-1})	ΔNH_2 (ν cm^{-1})	C=O (ν cm^{-1})	ΔC=O (ν cm^{-1})
6AFl (**3**)	3418, 3343, 3132	—	1642	—
[Cu(6AFl)$_2$$Cl_2$] (**3a**)	3258, 3123, 3074	160, 220, 58	1625	17
6AC (**4**)	3385, 3234, 3076	—	1617	—
[Cu(6AC)$_2$$Cl_2$] (**4a**)	3268, 3139, 3065	117, 95, 11	1616	1
[Ru(*p*-cymene)(6AC)Cl_2] (**4b**)	3218, 3136, 3066	167, 98, 10	1644	27

and reduction of Ru(II)/Ru(III). The separation between the anodic and cathodic peaks potentials is in the range 280–400 mV for copper-containing complexes, whereas ΔE_p is 84 mV for the ruthenium complex compound [Ru(*p*-cymene)(6AC)Cl_2] (**4b**). This indicates that the reduction and oxidation processes of Ru(III)/Ru(II) are easier than those of Cu(II)/Cu(I); however, the

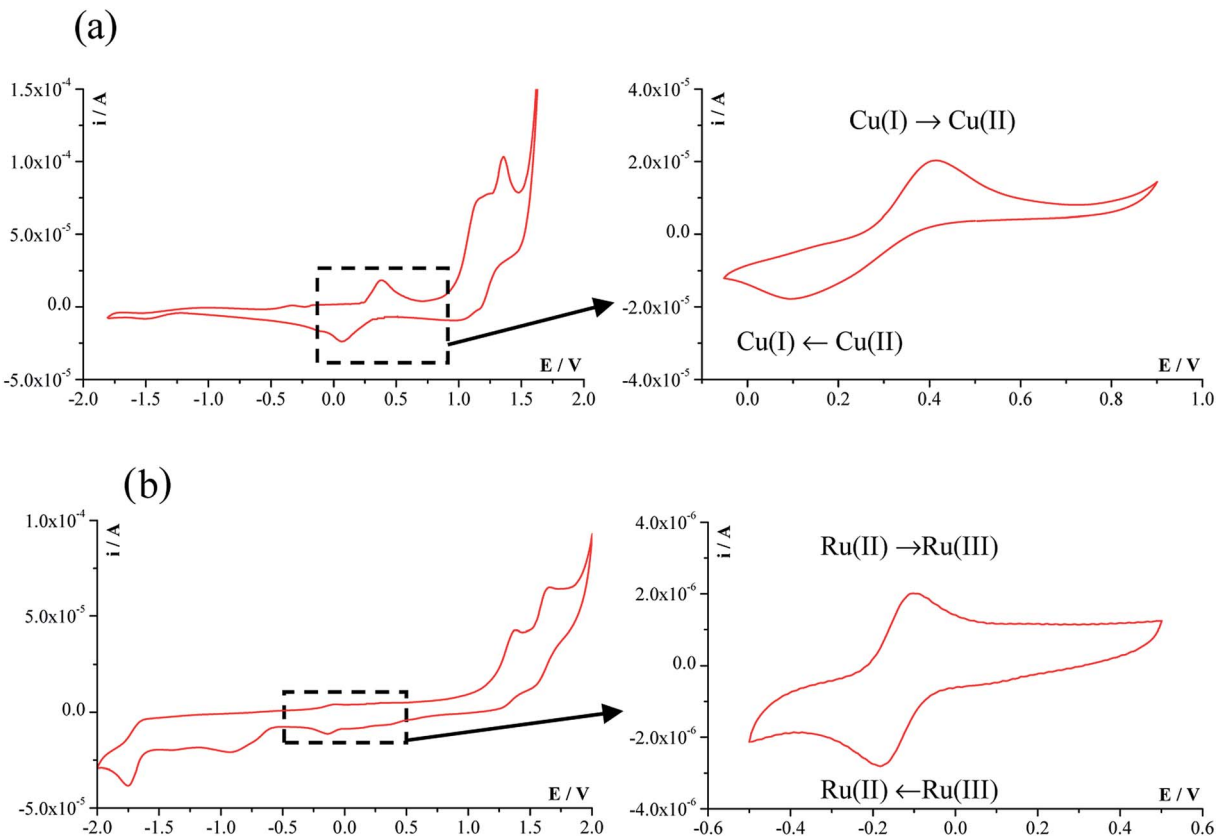

Fig. 3 CV voltammograms of (a) [Cu(7AFl)Cl_2] (**1a**) and (b) [Ru(*p*-cymene)(6AC)Cl_2] (**4b**).

Table 2 The potential–current parameters: cathodic peak potential (E_{pc}), anodic peak potential (E_{pa}), cathodic peak current (i_{pc}), anodic peak current (i_{pa}), ratio of anodic and cathodic peak currents (i_{pa}/i_{pc}) for copper-containing complexes (**1a–4a**) and [Ru(*p*-cymene)(6AC)Cl_2] (**4b**) compound

Compound	E_{pc} (V)	E_{pa} (V)	ΔE_p (V)	i_{pa}/i_{pc}
[Cu(7AFl)Cl_2] (**1a**)	0.070	0.383	0.313	0.88
[Cu(7A$_2$MC)$_2Cl_2$] (**2a**)	0.075	0.393	0.318	1.15
[Cu(6AFl)$_2Cl_2$] (**3a**)	0.095	0.378	0.283	1.16
[Cu(6AC)$_2Cl_2$] (**4a**)	0.026	0.427	0.401	1.18
[Ru(*p*-cymene)(6AC)Cl_2] (**4b**)	−0.098	−0.182	0.084	0.98

ruthenium(II) ion is chemically stable in the environment. The ratios of anodic and cathodic peak currents for the tested complexes compounds are close to 1, indicating that the redox processes are quasi-reversible.

2.6. Biological assays

The *in vitro* antitumor activity was determined in the human primary cancer cell lines WM 115 (Tumorigenic primary melanoma cell line), HL-60 (Human promyelocytic leukemia cells), NALM-6 (Human peripheral blood leukemia cells) and COLO 205 (Human caucasian colon adenocarcinoma) by means of colorimetric MTT assay. The MTT test is based on the ability of the mitochondrial enzymes of the living cells (mitochondrial dehydrogenase) to reduce the yellow, water-soluble tetrazole salt (3-(4,5-dimethylthiazol-2-yl) 2,5-diphenyltetrazolium bromide) to the insoluble purple formazan. After dissolving formazan crystals in DMSO, a colored product is formed, the amount of which ability is measured spectrophotometrically in the wavelength range 492–570 nm. The amount of colored reduced MTT is proportional to the oxidative activity of cell-mitochondria to the number of metabolically active (living) cells in the population. The MTT test is currently one of the most commonly used tests to evaluate the cytotoxic activity of compounds on metabolically active cells. Cells were exposed to broad range of drug concentration (10^{-7}; 10^{-6}; 10^{-5}; 10^{-4}; 10^{-3} M) for 48 hours. Naringenin, quercetin, cisplatin and carboplatin were used as the reference compounds. The concentration of DMSO did not exceed 0.1%.

The IC_{50} values against NALM-6 for all copper(II) complexes series are low: $IC_{50} = 39.7 \pm 3.7$ μM for complex **1a** and 36.5 ± 1.4 μM for complex **3a**. The strongest cytotoxic potency was found for complex **3a** ($IC_{50} = 29.2 \pm 3.5$ μM) against COLO-205 cells and is approximately twelve times better cytotoxic agent than carboplatin ($IC_{50} = 354.6 \pm 73.7$ μM) and two times better than cisplatin.

In general, the Ru(II) complexes presented herein, exhibit less cytotoxic effect in comparison to copper(II) complexes, given as IC_{50} values, expressed as μM units, in Table 3. Additionally all copper(II) complexes have lower IC_{50} values than their corresponding ligands, but only few ruthenium(II) complexes have the same properties. In most cases cytotoxic potency of Ru(II) complexes are lower than their corresponding ligands. Moreover both Cu(II) and Ru(II) complexes with 7- and 6-aminoflavones as ligands exhibit higher cytotoxic effect

Table 3 *In vitro* cytotoxicity of obtained complexes, in comparison to Naringenin, quercetin, cis- and carbo-platin with their IC_{50} values (μM) for 48 h challenge against various human tumor cells

	IC_{50} (μM)			
Compound	HL-60	NALM-6	WM 115	COLO 205
7AFl **1**	57.2 ± 2.0	54.5 ± 2.2	90.6 ± 5.4	73.1 ± 4.6
[Cu(7AFl)Cl_2] **1a**	37.8 ± 3.7	39.7 ± 3.7	68.0 ± 5.2	44.9 ± 4.5
[Ru(*p*-cymene)(7AFl)Cl_2] **1b**	79.0 ± 4.0	65.2 ± 1.3	412.1 ± 49.7	175.6 ± 29.0
[Ru(benzene)(7AFl)Cl_2] **1c**	140.7 ± 11.4	75.8 ± 3.7	474.2 ± 40.8	381.5 ± 44.4
[Ru(hexamethylbenzene)(7AFl)Cl_2] **1d**	91.2 ± 5.3	62.8 ± 2.9	334.5 ± 40.8	353.0 ± 37.3
7A2MC **2**	838.2 ± 33.2	591.3 ± 54.7	838.8 ± 30.7	774.1 ± 65.3
[Cu(7A2MC)$_2Cl_2$] **2a**	53.3 ± 3.3	51.8 ± 3.5	177.7 ± 28.7	64.6 ± 7.4
[Ru(*p*-cymene)(7A2MC)Cl_2] **2b**	395.7 ± 33.8	481.9 ± 51.7	497.8 ± 36.9	801.7 ± 70.9
6AFl **3**	272.4 ± 38.2	66.5 ± 5.3	699.1 ± 53.6	316.9 ± 30.4
[Cu(6AFl)$_2Cl_2$] **3a**	46.8 ± 4.9	36.5 ± 1.4	453.4 ± 29.9	29.2 ± 3.5
[Ru(*p*-cymene)(6AFl)Cl_2] **3b**	276.8 ± 37.2	67.0 ± 4.7	394.2 ± 26.2	406.4 ± 39.1
6AC **4**	779.8 ± 30.2	428.7 ± 28.2	>1000	>1000
[Cu(6AC)$_2Cl_2$] **4a**	62.7 ± 4.9	64.2 ± 4.1	>1000	73.6 ± 8.8
[Ru(*p*-cymene)(6AC)Cl_2] **4b**	505.2 ± 28.4	285.2 ± 33.4	617.1 ± 41.7	636.0 ± 20.6
Naringenin	413.7 ± 33.8	426.3 ± 20.5	524.8 ± 37.8	—
Quercetin	58.0 ± 4.0	77.1 ± 7.8	177.5 ± 21.5	—
Cisplatin	0.8 ± 0.1	0.7 ± 0.3	18.2 ± 4.3	61.45 ± 3.2
Carboplatin	4.3 ± 1.3	0.7 ± 0.2	422.2 ± 50.2	354.6 ± 73.7[a]

[a] IC_{50} values [μM] were calculated at concentration of a tested compound required to reduce the fraction of surviving cell to 50% of that observed in comparison to the control probe, non treated cell. Mean values are presented of parameter IC_{50} ± S.D. from 4 experiments.

against all cancer cell lines than corresponding complexes with 7-amino-2-methyl- and 6-aminochromone as ligands.

2.6.1. Generation of reactive oxygen species (ROS) and reactive nitrogen species (RNS). Reactive oxygen species (ROS) are a natural and inherent product of the aerobic metabolism of our cells. In physiological concentrations, they play an important role in the proper functioning of many cellular processes. ROS play the role of mediators in processes of cell growth, maturation and apoptosis, and influence inflammation and energy regulation in cells. Disturbances in the oxidative balance in cells can lead to damage to many cellular molecular components. It is believed that oxidative stress is the cause of many pathological conditions, or can occur during their course, and results in lipid and protein peroxidation or DNA damage. Attention is increasingly being paid to the role of ROS in the induction of apoptosis. Compounds that inhibit oxidative stress or cause it by generating ROS are increasingly used in anti-cancer therapy. The role of ROS in anticancer activity of many commonly used chemotherapy drugs including paclitaxel, docetaxel, cisplatin or doxorubicin, has already been documented. It has also been found that increased ROS levels are associated with the induction of mitochondrial damage and apoptosis.[21–23]

The molecular mechanisms behind the anticancer activity of the most active complexes was then examined using fluorimetric tests detecting the generation of free radicals: hydrogen peroxide, superoxide anion radical and nitric oxide. The amount of ROS (H_2O_2 and $O_2^{\bullet-}$) generated by investigated compounds was measured as well as the level of reactive nitrogen species (RNS). The cell cultures were incubated for 24 h with an IC_{50} concentration of derivatives **1**, **1a**, **1b**, **1c**, **1d**, **2a**, **3**, **3a**, **3b**, **4a** generated oxidative stress in NALM-6 (**1**, **1a**, **1b**, **1c**, **1d**, **2a**, **3**, **3a**, **3b**, **4a**), HL60 (**1**, **1a**, **1b**, **1d**, **2a**, **3a**, **4a**), WM115 (**1**, **1a**) and COLO205 (**1**, **1a**, **2a**, **3a**, **4a**).

The obtained results showed that the tested compounds can generate both H_2O_2 and $O_2^{\bullet-}$ and nitrogen species (NO). The level of ROS/RNS in cancer cells was dependent on their type and the chemical structure of the derivative (Fig. 4). In case of NALM cells, which were the most sensitive to the tested compounds, a marked increase in superoxide anion radical level was observed after incubation: approximately 15–25% increase in relation to untreated control cells. However, no statistically significant changes in the level of hydrogen peroxide were observed. The opposite situation was observed for the COLO205 cells, where the tested derivatives caused a significant increase in the level of hydrogen peroxide. Similar increases of about 10–20% *vs.* control cells were also observed for both the hydrogen peroxide and the superoxide anion levels in the case of the remaining two tumor cell lines: HL-60 and WM 115.

The investigated complexes also generate an appreciable amount of nitric oxide in cancer cells. As in the case of ROS, the generation of nitric oxide was correlated with the type of tumor cells and the compound used. Only in the case of the WM115 line were no statistically significant changes observed. HL-60 cells were the most sensitive: a 20–35% increase of NO was observed after the incubation with the investigated compounds. Slightly lower increase in RNS level (approximately 15–20%) was

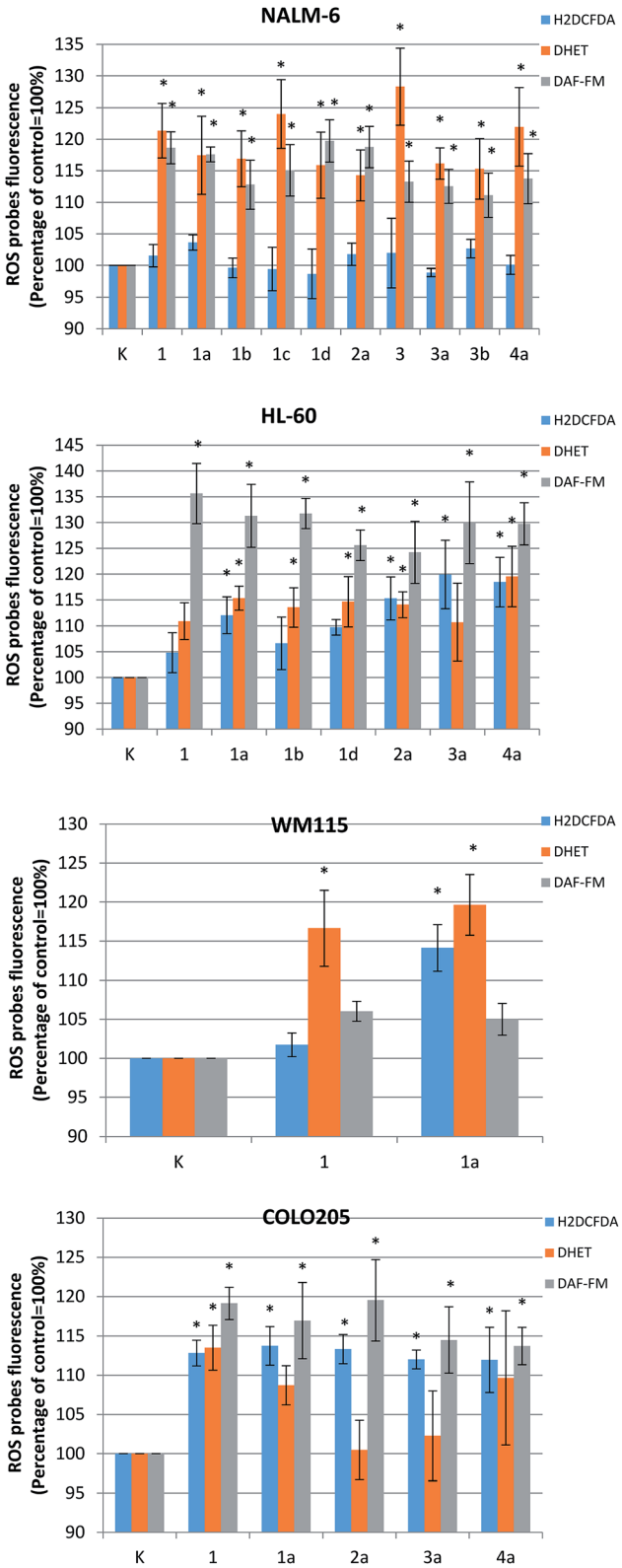

Fig. 4 Relative amounts of ROS/RNS generated in NALM-6, HL-60, WM 115 and COLO 205 cells by investigated compounds. The cells were incubated with IC_{50} concentration of complexes for 24 h and then the level of ROS/RNS was measured. The results represent mean ± SD of data from three individual experiments, each done at least in eight repeats; *$p < 0.05$ *versus* control.

observed for the other two tumor cell lines NALM-6 and COLO 205.

It was found that an increase in intracellular ROS level was associated with induction of mitochondrial damage and activation of the PCD pathway in tumor cells. Oxidative stress caused by the action of ruthenium(II) derivatives resulted in the amplification of apoptotic signals, which act through a number of intracellular signaling pathways comprising a range of proteins such as p53, and the MAPK kinase pathway.[24,25] Previous studies indicate that copper(II) compounds can cause ROS/RNS to generate mitochondrial dysfunction and oxidative DNA damage, which ultimately results in the activation of the mitochondrial apoptosis pathway among cancer cells.[26,27] In summary, our results are in agreement with those reported for several copper and ruthenium compounds, whose attractive anticancer activity is related to their ability to generate ROS/RNS in cancer cells.

3. Conclusions

The great challenge faced by modern oncology is the synthesis of effective and safe anticancer drugs that are characterized by high specificity of action against cancer cells. In recent years, there has been a significant increase in interest in the use of transition metal compounds as potential chemotherapeutic agents. The precursor of such compounds is the widely used cisplatin; however, its anticancer properties are also characterized by undesirable side effects. High hopes are associated with compounds containing ruthenium(II) or copper(II) in their structure.[28–30]

The present study compares and evaluates new N-coordinated copper(II) (**3a**, **4a**) and ruthenium(II) (**4b**) complexes synthesized as a complement of a previously described aminoflavone and aminochromone derivatives[19,20] as potential anticancer agents.

Cyclic voltammetry data indicated that the reduction and oxidation takes place more readily for Ru(III)/Ru(II) than for Cu(II)/Cu(I). These findings are important from the perspective of correct cell function, as the reduction potential of the cytoplasmic environment of the cell is −298 mV.[31] It can be concluded that the oxidation and reduction processes of the tested complexes compounds may occur *in vivo*.

To evaluate the significance of oxidative stress in the cytotoxic effects of the ruthenium(II) and copper(II) complexes against human cancer cell lines and to investigate their molecular anticancer activity, the levels of generated ROS (H_2O_2 and $O_2^{\bullet-}$) and RNS (NO) were measured. Preliminary analysis found some compounds to have higher cytotoxic potency towards HL-60, NALM-6, WM 115 and COLO 205 cells than standard referential compounds. They cause an increase of ROS/RNS in cancer cells, and it seems likely that the pro-oxidative properties of the tested compounds correlate with their chemical structure (SAR – structure activity relationship).

The obtained results provide an introduction to the analysis of the antitumor activity of transition metal derivatives. In the future we hope to investigate the molecular mechanisms of described complexes' activity in human cancer cells that could be responsible for: (I) the induction of apoptosis; (II) generation of oxidative stress and (III) genotoxicity of these compounds. Understanding the molecular pathways responsible for the antitumor activity of these molecules and their structure–activity interrelationships (SAR) is essential for the further development of chemotherapy and the improvement of the synthesis of new compounds with even greater anticancer properties.

4. Experimental

4.1. Material and methods

Most obtained complexes were synthesized according to Pastuszko *et al.* and Mucha *et al.*[19,20] The synthesis and physicochemical properties of the new compounds, $[Cu(6AFl)_2Cl_2]$ (**3a**), $[Cu(6AC)_2Cl_2]$ (**4a**) and [Ru(*p*-cymene)(6AC)Cl_2] (**4b**) are described below. The reactants and solvents used in this work were reagent grade or better. They were purchased from Sigma-Aldrich, Chempur and POCH chemical companies and used without further purification. The samples were dried according to standard methods.

Melting points were determined using a Buchi Melting Point B540 apparatus and are uncorrected. The infrared transmission spectra of crystalline products were recorded using a Mattson Infinity MI-60 spectrophotometer in KBr and a Nicolet iS50 FT-IR spectrophotometer equipped with a Specac Quest single-reflection diamond attenuated total reflectance (ATR) accessory. Spectral analysis was controlled by the OMNIC software package. Elemental analyses was obtained in the Microanalytical Laboratory of the Department of Bioorganic Chemistry (Medical University, Lodz) using a PerkinElmer PE 2400 CHNS analyzer. ^{1}H and ^{13}C-NMR spectra was measured on a Bruker Avance III (600 MHz) instrument in DMSO-d_6; chemical shifts (δ) are given in ppm, coupling constants (J) in Hz. ^{1}H-NMR data are presented as follows: chemical shift, multiplicity (br = broad, s = singlet, d = doublet, dd = doublet doublet), coupling constant, integration. The mass spectra were recorded on a Finnigan MAT-95 and the Varian 500-MS LC Ion Trap mass spectrometer (ESI).

4.2. Synthesis of 6-amino-2-phenyl-4*H*-1-benzopyran-4-one copper complex $[Cu(6AFl)_2Cl_2]$ (3a)

6-Amino-2-phenyl-4*H*-1-benzopyran-4-one (**3**) (47.45 mg, 0.2 mmol) was heat-dissolved in ethyl acetate (10 mL). A solution of copper(II) chloride dihydrate $CuCl_2 \cdot 2H_2O$ (17.04 mg, 0.1 mmol) in methanol (1 ml) was added dropwise to a mixing solution of ligand. The reaction mixture was stirred at room temperature for 24 h and a dark yellow precipitate was obtained. The solid was filtered off, washed with diethyl ether and dried in the air. Yield: 48.49 mg (78%). Mp 208–213 °C. IR (KBr): ν (cm^{-1}) 3258 m, 3123 m, 3074 m, 1625 s, 1583 s, 1569 s, 1557 s, 1497 s, 1484 s, 1386 m, 1076 m, 909 m, 855 m, 810 m, 764 m, 674 m, 651 m. Anal. calc $C_{30}H_{22}N_2O_4CuCl_2 \cdot 0.5H_2O$ (M = 617.91 g mol^{-1}) anal. (%): C 58.30; H 3.75; N 4.53. Found (%): C 58.61; H 3.12; N 4.56. ESI-MS (m/z): 572.0 $[2Cu(6AFl)Cl–H]^+$.

4.3. Synthesis of 6-amino-4*H*-1-benzopyran-4-one copper complex [Cu(6AC)$_2$Cl$_2$] (4a)

6-Amino-4*H*-1-benzopyran-4-one (**4**) (32.23 mg, 0.2 mmol) was heat-dissolved in ethyl acetate (10 mL). A solution of copper(II) chloride dihydrate $CuCl_2 \cdot 2H_2O$ (17.04 mg, 0.1 mmol) in methanol (1 ml) was added dropwise to a mixing solution of ligand. The reaction mixture was stirred at room temperature for 24 h and a brown precipitate was obtained. The solid was filtered off, washed with diethyl ether and dried in the air. Yield: 30.15 mg (66%). Mp 152–153 °C. IR (KBr): ν (cm^{-1}) 3268, 3139, 3065, 1616, 1591, 1571, 1472, 1318, 1265, 1064, 831 $C_{18}H_{14}N_2O_4CuCl_2$ (M = 456.79 g mol^{-1}): Anal. (%): C 47.33; H 3.10; N: 6.13. Found (%): C 48.19; H 2.55; N 6.18. ESI-MS (m/z): 420.0 [2Cu(6AC)Cl–H]$^+$.

4.4. Synthesis of [Ru(η^6-*p*-cymene)(6-amino-4*H*-1-benzopyran-4-one-κ^1-*N*)Cl$_2$] [Ru(*p*-cymene)(6AC)Cl$_2$] (4b)

While stirring a solution of 6-amino-4*H*-1-benzopyran-4-one (**4**) (32.24 mg; 0.2 mmol) in chloroform (6 mL) and 6 mL of methanol, a solution of [Ru(η^6-*p*-cymene)Cl$_2$]$_2$ (**b**) (61.24 mg; 0.1 mmol) in 6 mL of CH_2Cl_2 was added dropwise under an argon atmosphere. The mixture was stirred for 24 hours at room temperature. The solution was concentrated under reduced pressure and the obtained red-orange precipitate was washed with diethyl ether and dried under reduced pressure. Yield: 72.0 mg (75.63%), and dec.: 210.6 °C. IR (KBr): ν (cm^{-1}) 3218 m, 3136 m, 3066 m, 1644 s, 1575 s, 1483 s, 884 m, 862 m, 840 m. ^{1}H NMR (600 MHz, DMSO-d$_6$) δ (ppm): 1.19 (d, 6H, *p*-cymene, CH–(C**H**$_3$)$_2$, $^3J_{HH}$ = 12 Hz); 2.09 (s, C**H**$_3$, 3H, *p*-cymene); 2.84 (septet, 1H, C**H**–(CH$_3$)$_2$, *p*-cymen), $^3J_{HH}$ = 6 Hz); 5.45 (s, 2H, N**H**$_2$, Ar$_{chromone}$); 5.77 (d, 2 × **H**$_{2(AA')}$, *p*-cymene, $^3J_{HH}$ = 6 Hz); 5.81 (d, 2 × **H**$_{3(BB')}$, *p*-cymene, $^3J_{HH}$ = 6 Hz); 7.03 (dd, 1H, Ar$_{chromone}$, $^3J_{HH}$ = 12 Hz); 7.08 (d, 1H, Ar$_{chromone}$, $^3J_{HH}$ = 6 Hz); 7.34 (d, 1H, Ar$_{chromone}$, $^3J_{HH}$ = 12 Hz); 8.13 (d, 1H, Ar$_{chromone}$, $^3J_{HH}$ = 6 Hz).^{13}C NMR (600 MHz, DMSO-d$_6$) δ (ppm): 18.35 (**C**H$_3$, *p*-cymene), 21.97 (2 × **C**H$_3$, *p*-cymene), 30.45 (**C**H, *p*-cymene), 85.98, 86.83, 100.54, 105.33 (4 × **C**H, Ar$_{chromone}$), 106.82 (**C**, Ar$_{chromone}$), 111.35 (2 × **C**H, Ar$_{p\text{-}cymene}$), 119.36 (2 × **C**H, Ar$_{p\text{-}cymene}$), 122.11, 126.08 (2 × **C**, Ar$_{p\text{-}cymene}$), 147.03 (**C**NH$_2$, Ar$_{chromone}$) 148.68 (**C**, Ar$_{chromone}$) 156.45 (**C**, Ar$_{chromone}$), 176.89 (**C**=O, Ar$_{chromone}$). Anal. calc. $C_{19}H_{21}Cl_2NO_2Ru \cdot 0.5H_2O$ (M = 476.35 g mol^{-1}) anal (%): C 47.86; H 4.62; N 2.93. Found (%): C 47.59; H 4.73; N 2.96. ESI-MS (m/z): 468.2 [Ru(*p*-cymene(6AC)Cl$_2$]$^+$.

4.5. Redox properties

Cyclic voltammetry (CV) technique were employed to determine the electrochemical properties of complexes with Cu(II) ions. The studies were performed in 0.1 M [nBu$_4$N][BF$_4$] in DMF as the supporting electrolyte. All voltammetric measurements carried out using a potentiostat/galvanostat Autolab PGSTAT128N (Metrohm Autolab B. V., Utrecht, the Netherlands) controlled by a personal computer with GPES software (version 4.9) and an M164 electrode stand (MTM Anko Instruments, Krakow, Poland) at room temperature. A platinum wire was used as the counter electrode, and a silver wire as the pseudo-reference electrode. A glassy carbon (GCE, L-Chem, Olomouc-Holice, the Czech Republic) with 3 mm diameter was used as the working electrode. The GCE surface was refined using 0.3 μm Al_2O_3 slurry (ATM GMBH, Germany), rinsed with triply distilled water, ultrasonically treated for 10 min and dried with argon. Before each measurement all solutions were deoxygenated for 20 min with argon (5 N, Air Liquide, Poland) and then maintaining argon atmosphere over the solution during the measurement.

4.6. Cell cultures and cytotoxicity assay by MTT

Cytotoxicity was tested against human skin melanoma WM-115 cells, and human leukemic promyelocytic HL-60 and lymphoblastic NALM-6 cell lines and human Caucasian colon adenocarcinoma COLO 205. The cell lines (WM-115, COLO-205 and HL-60) used in the work came from ATCC American Type Culture Collection (Rockville, Manassas, VA, USA), whereas NALM-6 cell line was purchased from the German Collection of Microorganisms and Cell Cultures. The leukaemia cells were cultured in RPMI 1640 medium (Thermo Fisher Scientific, Waltham, Massachusetts, USA) supplemented with 10% fetal bovine serum and antibiotic (gentamicin 25 μg ml^{-1}) (Gibco, Grand Island, New York, NY, USA). For melanoma WM-115 cells, Dulbecco's minimal essential medium (DMEM, Lonza, Visp, Switzerland) instead of RPMI 1640 was used. Cells were grown at 37 °C in a humidified atmosphere of 5% CO_2 in air.

The cytotoxicity of all obtained compounds, and the four reference compounds was determined by the MTT [3-(4,5-dimethylthiazol-2-yl)-2,5-diphenyltetrazolium bromide, Sigma, St. Louis, MO] assay as described elsewhere.[32] Briefly, after 46 h of incubation with the test compounds, the cells were treated with the MTT reagent and incubation was continued for another two hours. MTT – formazan crystals were dissolved in 20% SDS and 50% DMF at pH 4.7 and absorbance was read at 562 and 630 nm on a multifunctional Victor ELISA-plate reader[3] (PerkinElmer, Turku, Finland). The IC_{50} values, *i.e.* the concentration of the test compound required to reduce the cell survival fraction to 50% of controls, were calculated from concentration–response curves and used as a measure of the sensitivity of the cells to a given treatment. Cytotoxicity toward HL-60, NALM-6, WM 115 and COLO 205 was determined for five different concentration of the studied compounds 10^{-7}; 10^{-6}; 10^{-5}; 10^{-4} and 10^{-3} M. As a control, cultured cells were grown in the absence of drugs. The data points represent the means of at least five to 10 repeats ± SD

4.7. Reactive oxygen species (ROS) measurement

The level of reactive oxygen species in cancer cell lines was determined by spectrophotometric microplate method using two oxidation-sensitive fluorescent probes: 2′,7′-dichlorodihydrofluorescein diacetate (H2DCF-DA, Sigma-Aldrich, St. Louis, MO, USA), dihydroethidium (DHE, Cayman Chemical Company, Michigan, USA) which may react with several ROS. The cell-permeant non-fluorescent dye H_2DCF-DA is diffused into cells, where it is deacetylated by cellular esterases and oxidized to highly fluorescent 2′,7′-dichlorodihydroflourescein (DCF) by ROS ($\lambda_{ex}/\lambda_{em}$: 498/525 nm). The DHE fluorescence probe also has the ability to permeate cell membranes and is

mainly used to monitor superoxide production. DHE itself shows blue fluorescence, but in the cell cytoplasm it is oxidized by super-oxide to 2-hydroxyethidium, which becomes red fluorescent upon DNA intercalation. Cells were seeded in a black 96-well fluorimetric microplates at a density of 15×10^3 cells per well 24 hours before the treatment. Cells were incubated with the investigated compounds (IC_{50} concentration) for 24 hours. After incubation cells were centrifuged at 1000 rpm for five minutes at 4 °C. The medium was removed and 50 μl of HBSS buffer containing H_2DCF-DA or DHE (final concentration 5 μM) was added to each well. The cells were incubated with the fluorescent probes for 30 min in a CO_2 incubator, in a dark at 37 °C and the DCF/DHE fluorescence was measured.

4.8. Reactive nitrogen species (RNS) measurement

4-Amino-5-methylamino-2′,7′-difluorofluorescein diacetate (DAF-FM Diacetate, Invitrogen, Carlsbad, USA) was applied to measure RNS production in investigated cancer cells. DAF-FM is a redox-sensitive fluorescent probe that is used to detect and quantify low concentrations of nitric oxide (NO). It is essentially non fluorescent until it reacts with NO to form a fluorescent benzotriazole ($\lambda_{ex}/\lambda_{em}$: 495/515 nm). The procedure was similar to that described above for ROS measurement. Monolayers of treated and control cells seeded into black flat-bottom 96-well microplates after incubation with investigated compounds were centrifuged. Then DAF-FM in 50 mL HBSS (final concentration 5 μM) was added to each well. The cells were incubated with the fluorescent probes for 30 min in a CO_2 incubator, in a dark at 37 °C. After incubation the probe was removed and replace with fresh HBSS buffer, and then incubated for an additional 30 minutes to allow complete de-esterification of the intracellular diacetates. Fluorescence excitation and emission maxima are 495 and 515 nm, respectively.

4.9. Statistical analysis

All data are expressed as the mean SD and presented as a percentage of control (untreated cells) taken as 100%. Normality of data was tested with the Shapiro–Wilk test, and homogeneity of variance was verified with Levene's test. The significance of the differences between pairs of means was estimated using one-way ANOVA and the *posthoc* Tukey's test. All statistics were calculated with the STATISTICA statistical software package (StatSoft, Tulsa, OK, USA). A $*p$ value of <0.05 was considered significant.

Conflicts of interest

There are no conflicts to declare.

Acknowledgements

Financial support from grant No 503/3-066-02/503-31-001 to Prof. Elzbieta Budzisz at Medical University of Lodz is gratefully acknowledged. We are grateful to Dr Adam Pastuszko and Dr Anna Skoczyńska for their help in the synthesis of ruthenium(II) complexes.

References

1 F. Perez-Vizcaino and C. G. Fraga, Research trends in flavonoids and health, *Arch. Biochem. Biophys.*, 2018, **646**, 107–112.
2 M. Abotaleb, S. M. Samuel, E. Varghese, S. Varghese, P. Kubatka, A. Liskova and D. Büsselberg, Flavonoids in cancer and apoptosis, *Cancers*, 2019, **11**, 28, DOI: 10.3390/cancers11010028.
3 A. Gaspar, M. J. Matos, J. Garrido, E. Uriarte and F. Borges, Chromone: a valid scaffold in medicinal chemistry, *Chem. Rev.*, 2014, **114**, 4960–4992.
4 J. Reis, A. Gaspar, N. Milhazes and F. Borges, Chromone as a privileged scaffold in drug discovery: recent advances, *J. Med. Chem.*, 2017, **60**, 7941–7957.
5 A. L. Laine and C. Passirani, Novel metal-based anticancer drugs: a new challenge in drug delivery, *Curr. Opin. Pharmacol.*, 2012, **12**, 420–426.
6 T. Zou, C. T. Lum, C.-N. Lok, J.-J. Zhang and C.-M. Che, Chemical biology of anticancer gold(III) and gold(I) complexes, *Chem. Soc. Rev.*, 2015, **44**, 8786–8801.
7 J. P. C. Coverdale, T. Laroiya-McCarron and I. Romero-Canelon, Designing Ruthenium Anticancer Drugs: What Have We Learnt from the Key Drug Candidates?, *Inorganics*, 2019, **7**(3), 31.
8 C. Marzano, M. Pellei, F. Tisato and C. Santini, Copper Complexes as Anticancer Agents, *Anti-Cancer Agents Med. Chem.*, 2009, **9**, 185–211.
9 I. Bertini, *Biological Inorganic Chemistry: Structure and Reactivity*, University Science Books, Sausalito, CA, 2007.
10 E. Gaggelli, F. Bernardi, E. Molteni, R. Pogni, D. Valensin, G. Valensin, M. Remelli, M. Luczkowski and H. Kozlowski, Interaction of the human prion PrP(106-126) sequence with copper(II), manganese(II), and zinc(II): NMR and EPR studies, *J. Am. Chem. Soc.*, 2005, **127**, 996–1006.
11 A. Ramdass, V. Sathish, E. Babu, M. Velayudham, P. Thanasekaran and S. Rajagopal, Recent developments on optical and electrochemical sensing of copper(II) ion based on transition metal complexes, *Coord. Chem. Rev.*, 2017, **343**, 278–307.
12 S. Eghbaliferiz and M. Iranshahi, Prooxidant Activity of Polyphenols, Flavonoids, Anthocyanins and Carotenoids: Updated Review of Mechanisms and Catalyzing Metals, *Phytother. Res.*, 2016, **30**, 1379–1391.
13 D. Procházková, I. Boušová and N. Wilhelmová, Antioxidant and prooxidant properties of flavonoids, *Fitoterapia*, 2011, **82**, 513–523.
14 J. Qi, S. Liang, Y. Gou, Z. Zhang, Z. Zhou, F. Yang and H. Liang, Synthesis of four binuclear copper(II) complexes: structure, anticancer properties and anticancer mechanism, *Eur. J. Med. Chem.*, 2015, **96**, 360–368.
15 H. Kozlowski, M. Luczkowski, M. Remelli and D. Valensin, Copper, zinc and iron in neurodegenerative diseases (Alzheimer's, Parkinson's and prion diseases), *Coord. Chem. Rev.*, 2012, **256**, 2129–2141.

16 C. S. Allardyce and P. J. Dyson, Ruthenium in Medicine: Current Clinical Uses and Future Prospects, *Platinum Met. Rev.*, 2001, **45**, 62–69.
17 C. S. Allardyce, A. Dorcier, C. Scolardo and P. J. Dyson, Development of organometallic (organo-transition metal) pharmaceuticals, *Appl. Organomet. Chem.*, 2005, **19**, 1–10.
18 W. H. Ang and P. J. Dyson, Classical and Non-Classical Ruthenium-Based Anticancer Drugs: Towards Targeted Chemotherapy, *Eur. J. Inorg. Chem.*, 2006, 4003–4018.
19 P. Mucha, M. Małecka, B. Kupcewicz, K. Lux, A. Dołęga, J. Jezierska and E. Budzisz, Copper(II) complexes of 7-amino-2-methylchromone and 7-aminoflavone: magneto-structural, spectroscopic and DFT characterization, *Polyhedron*, 2018, **153**, 181–196.
20 A. Pastuszko, K. Majchrzak, M. Czyz, B. Kupcewicz and E. Budzisz, The synthesis, lipophilicity and cytotoxic effects of new ruthenium(II) arene complexes with chromone derivatives, *J. Inorg. Biochem.*, 2016, **159**, 133–141.
21 D. Trachootham, J. Alexandre and P. Huang, Targeting cancer cells by ROS-mediated mechanisms: a radical therapeutic approach?, *Nat. Rev. Drug Discovery*, 2009, **8**, 579–591.
22 X. Peng and V. Gandhi, ROS-activated anticancer pro drugs: a new strategy for tumor-specific damage, *Ther. Delivery*, 2012, **3**, 823–833.
23 C. Martin-Cordero, A. J. Leon-Gonzalez, J. M. Calderon-Montano, E. Burgos-Moron and M. Lopez-Lazaro, Pro-oxidant natural products as anticancer agents, *Curr. Drug Targets*, 2012, **13**, 1006–1028.
24 Z. Zhao, Z. Luo, Q. Wu, W. Zheng, Y. Feng and T. Chen, Mixed-ligand ruthenium polypyridyl complexes as apoptosis inducers in cancer cells, the cellular translocation and the important role of ROS-mediated signaling, *Dalton Trans.*, 2014, **43**, 16947–17212.
25 G.-B. Jiang, J.-H. Yao, J. Wang, W. Li, B.-J. Han, Y.-Y. Xie, G.-J. Lin, H.-L. Huang and Y.-J. Liu, The induction of apoptosis in BEL-7402 cells through the ROS-mediated mitochondrial pathway by a ruthenium(II) polypyridyl complex, *New J. Chem.*, 2014, **38**, 2554–2563.
26 C. Acilan, B. Cevatemre, Z. Adiguzel, D. Karakas, E. Ulukaya, N. Ribeiro, I. Correia and J. C. Pessoa, Synthesis, biological characterization and evaluation of molecular mechanisms of novel copper complexes as anticancer agents, *Biochim. Biophys. Acta*, 2017, **1861**, 218–234.
27 D. Denoyer, S. A. S. Clathorthy and M. A. Cater, Copper complexes in cancer therapy, *Met. Ions Life Sci.*, 2018, **18**, 469–506.
28 N. P. E. Barry and P. J. Sadler, Challenges for Metals in Medicine: How Nanotechnology May Help To Shape the Future, *ACS Nano*, 2013, **7**, 5654–5659.
29 A. Monney and M. Albrecht, Transition metal bioconjugates with an organometallic link between the metal and the biomolecular scaffold, *Coord. Chem. Rev.*, 2013, **257**, 2420–2433.
30 G. Gasser and N. Metzler-Nolte, The potential of organometallic complexes in medicinal chemistry, *Curr. Opin. Chem. Biol.*, 2012, **16**, 84–91.
31 M. D. Hall, T. W. Failes, N. Yamamoto and T. W. Hambley, Bioreductive activation and drug chaperoning in cobalt pharmaceuticals, *Dalton Trans.*, 2007, **36**, 3983–3990.
32 P. C. Hariharan and J. A. Pople, The influence of polarization functions on molecular orbital hydrogenation energies, *Theor. Chim. Acta*, 1973, **28**, 213–222.